Immunopathologia Persa
DOI:10.34172/ipp.2025.42735
http immunopathol.com

$C_{20}H_{13}ClFN_3O$ p38 MAPK inhibitor decreases the expression of NF-kB p65 and suppresses breast cancer cell growth; an *in-vitro* study

Mustafa Abduljabbar A-qader[1*], Intesar Tarik Numan[2], Basma Talib Al-Sudani[1]

[1]College of Pharmacy, Department of Pharmacology and Toxicology, Mustansiriyah University, Baghdad, Iraq
[2]Al-Nukhba University College, Department of Pharmacy, Baghdad, Iraq

***Correspondence to**
Mustafa Abduljabbar A-qader,
Email: mustafa_a.aljabbar@uomustansiriyah.edu.iq

Received 13 Aug. 2024
Revised: 10 Nov. 2025
Accepted 16 Nov. 2025
ePublished 24 Feb. 2026

Keywords: Nuclear factor kappa B, Breast cancer, Cell cycle arrest, Apoptosis, Western blot

Abstract

Introduction: Breast cancer is the second most common cause of cancer-related deaths among women globally. Mitogen-activated protein kinases (MAPKs) are serine/threonine kinases with diverse cellular response functions. Additionally, p38 activation has been demonstrated in response to several external stimuli, including ultraviolet light, heat, osmotic shock, inflammatory cytokines, and growth factors. In this study, $C_{20}H_{13}ClFN_3O$ compound's cytotoxicity effect, apoptosis, and cell cycle arrest in MDA-MB-231 and MCF-7 cells were evaluated.
Objectives: To evaluate the potential of $C_{20}H_{13}ClFN_3O$ compound as a p38 MAPK inhibitor for treating breast cancer.
Materials and Methods: This experimental study was conducted *in-vitro* to assess the anti-proliferative and apoptotic effects of $C_{20}H_{13}ClFN_3O$ compounds on MDA-MB-231 and MCF-7 cells.
Results: The cytotoxicity assay showed that the half maximal inhibitory concentration of $C_{20}H_{13}ClFN_3O$ in MCF-7 cells was 5.355 µg, and in MDA-MB-231 cells was 1.419 µg. In the FITC-annexin V apoptosis by flow cytometry in MCF-7 cells, the compound led to an increased early apoptotic by 70%. In contrast, in MDA-MB-231 cells, the compound led to a 23% increase in the early apoptotic effect. Furthermore, western blot results showed decreased p38 and NF-κB protein expression in both cell lines when treated with the compound.
Conclusion: In our study, the compound $C_{20}H_{13}ClFN_3O$ that inhibits the p38 pathway shows promise as a new cancer treatment target. This study suggests that $C_{20}H_{13}ClFN_3O$ could be a therapeutic target for breast cancer.

Citation: Abduljabbar A-qader M, Numan IT, Talib Al-Sudani B. $C_{20}H_{13}ClFN_3O$ p38 MAPK inhibitor decreases the expression of NF-kB p65 and suppresses breast cancer cell growth; an *in-vitro* study. Immunopathol Persa. 2026;x(x):e42735. DOI:10.34172/ipp.2025.42735.

Introduction

Breast cancer is the most common malignancy in women worldwide, accounting for 25% of all cancers (1). Breast cancer is the most common cancer and the second leading cause of cancer-related death in women worldwide (2). Invasive breast cancer remains the leading cancer in women worldwide, accounting for approximately 11.7% of newly diagnosed cases in 2020 (3). The incidence of new cancers in Iraq has been increasing, from 52.00 per 100,000 people in 2000 to 91.66 per 100,000 people in 2019. In 2019, breast cancer was the leading cause of death in Iraqi women, accounting for approximately one-third of all recorded cancer cases in the country. In addition, its incidence (22.58%) and mortality (6.22 per 100,000 people) are also the highest among all cancers (4). Breast cancer is a clinically heterogeneous disease with high mortality and morbidity rates worldwide (5). This malignancy can be hereditary and is caused by radiation exposure, toxic environmental influences, alcohol consumption, and lifestyle (6). Metastasis (including migration and invasion) is the main cause of death in cancer patients (7). Therefore, it is very important to inhibit the migration and invasion of cancer cells (8). Breast cancer is divided into different subtypes based on the endocrine expression levels of progesterone receptor (PR), human epidermal growth receptor (HER2), and estrogen receptor (ER), which differ in morphology and clinical features (9). Approximately 15%-20% of breast cancers are triple-negative breast cancer (TNBC), which is negative for estrogen, progesterone, and HER2 receptors (10). Clinically, TNBC is characterized by poor prognosis, high proliferation and invasiveness of cancer cells, and rapid development compared with other types of breast cancer (11). The molecular mechanisms of TNBC are not yet fully understood (12). In addition, it is necessary to understand the molecular mechanisms of TNBC and explore effective therapeutic targets.

Key point

The compound $C_{20}H_{13}ClFN_3O$ has the potential as a therapeutic target for breast cancer by inhibiting the p38 MAP kinase pathway. In our study, $C_{20}H_{13}ClFN_3O$ shows significant cytotoxic effects, induces apoptosis, causes cell cycle arrest in the synthesis phase, and reduces the expression of p38 and NF-κB p65 proteins in MCF-7 and MDA-MB-231 breast cancer cell lines.

Mitogen-activated protein kinases (MAPKs) are Ser/Thr kinases that have multiple functions in the response of cells to various stimuli, such as mitogens, osmotic pressure, heat shock, and proinflammatory cytokines. MAPKs play vital roles in various biological processes, including proliferation, gene expression, differentiation, mitosis, cell survival, and cell death (13). There are four major MAPKs in mammals: (1) ERK1/2, (2) c-Jun N-terminal kinase (JNK)1–3, (3) p38, and ERK5 (4). Researchers worldwide regularly study the key functions of ERK1 and ERK2 in cell proliferation and survival. JNK and p38 MAPK signaling pathways primarily involve cellular stress responses and apoptosis regulation (14).

Meanwhile, p38 activation has been demonstrated in response to several external stimuli, including ultraviolet (UV) light, heat, osmotic shock, inflammatory cytokines (TNF-alpha and IL-1), and growth factors (CSF-1). Moreover, the activation of p38 is contingent not only on the stimuli but also on the specific cell type (15). Meanwhile, P38 has little reactivity in its non-phosphorylated state, but it rapidly becomes activated upon phosphorylation of two Thr-Gly-Tyr motifs. Similar to other MAPKs, p38 is activated by dual kinases called MKKs. Upregulation of MKK kinases leads to the activation of both p38 and JNK pathways (16). Cellular responses vary significantly depending on the particular cell type and the stimulus received. Due to these properties, the role of p38 in cancer development and treatment is complex. Elevated levels of p38 are associated with aggressiveness and adverse outcomes in breast cancer (17).

Likewise, nuclear factor kappa B (NF-κB) is a protein complex that plays a crucial role in cancer research because it regulates the transcription of many genes. Substances produced by these genes promote cell survival by inhibiting the apoptotic process in both healthy and malignant cells (18). It promotes DNA binding, dimerization, and interaction with inhibitors called inhibitors of kappa B (IKK) (19). Dimeric IKK consists of two kinase subunits, IKKα and IKKβ, which are similar. These inhibitors prevent NF-κB dimers (p50/p65) from entering the cytoplasm. However, upon phosphorylation and degradation of the IKK protein, NF-κB is released, allowing the dimers to enter the nucleus (20). Prior studies showed that NF-κB promotes cell cycle progression by regulating the function of genes associated with the cell cycle system. Expression of cyclin D1, a protein that plays a key role in regulating the cell cycle. It is a member of the cyclin family and is involved in the control of cell cycle progression. It is generated by NF-κB and is particularly important for mammary gland development and the development of breast cancer (21). This cell cycle regulator is important because it forms active complexes with its binding partners (cyclin-dependent kinases 4 and 6). These complexes promote the transition from the G1 phase (gap 1) to the synthetic phase by adding phosphate groups to the retinoblastoma protein and inactivating it (21). Currently, the role of the NF-κB signaling pathway in cellular biological activity is a hot topic in cancer research. The NF-κB signaling pathway plays a crucial role in various physiological processes such as immune response, inflammation, and stress response, as well as in the regulation of cell differentiation, proliferation, and programmed cell death (apoptosis) (22). The NF-κB signaling pathway is frequently altered in solid tumors and hematopoietic malignancies, thereby stimulating the growth and survival of tumor cells. Recent studies have shown that NF-κB has a tumor suppressor function in certain cancers through the activation of Fas ligand by transcriptional processes (23). Studies have also demonstrated a complex interaction between NF-κB and p38 (24). The association between these two factors has been shown to be essential for the activation of the interleukin 6 gene (25). This gene's protein product is often elevated in patients with metastatic cancer (26). Inhibition of the p38 protein reduces the expression of NF-κB-targeted genes and decreases NF-κB-driven transcriptional (27). As there are few effective treatments for breast cancer and it is a major global health problem, there is an urgent need to focus on the discovery of new treatment options. One promising research approach is the development of p38 MAP kinase inhibitors as potential cancer treatments. These inhibitors show great potential in affecting specific signaling pathways involved in cancer development, making them promising candidates for treating the aggressive nature of breast cancer, especially in subtypes such as TNBC. Enhanced research and development in this area could lead to more effective treatment strategies, improving patient outcomes and reducing the global burden of breast cancer. The current study showed that the $C_{20}H_{13}ClFN_3O$ compound effectively inhibited cell growth at lower concentrations, indicating less toxicity to healthy cells also, this study found the relationship between two biomarkers (p38 and NF-κB). Therefore, the findings provide unique directions for further investigation that can expand upon current work.

Objectives

To evaluate the potential of the P38 MAP kinase inhibitor 2-(4 chlorophenyl)-4-(4-fluorophenyl)-5-pyridin-4-yl-1,2-dihydropyrazol-3-one compound as a p38 MAP kinase inhibitor for treatment against breast cancer by study the cytotoxicity effect, apoptosis and cell cycle arrest of this compound in MDA-MB-231 and MCF-7 cells as a model for breast cancer as well as study the protein expression of

the p38 MAP kinase and NF-κB p6 proteins after treating the breast cancer cells with $C_{20}H_{13}ClFN_3O$ compound by western blot assay.

Materials and Methods

Chemicals and reagents

The $C_{20}H_{13}ClFN_3O$ compound (Santa Cruz Biotechnology), lapatinib (Macklin, Shanghai, China). The following were obtained from Elabscience (USA); an annexin V/PI detection kit, a cell cycle assay kit (red fluorescence), SDS-PAGE gel kit, a trypan blue 0.4%, and a western blot detection kit.

High glucose (4.5 g/L) Dulbecco's modified eagle's medium (DMEM) with stable glutamine and 25 mM HEPES, fetal bovine serum 10% (FBS), phosphate buffer saline (PBS), trypsin-EDTA 0.05 % solution, and antibiotic/antimycotic solution (10x) were obtained from (Capricorn Scientific, Germany). MTT reagent (3-(4,5-dimethylthiazol-2-yl)-2,5-diphenyl-2H-tetrazolium bromide) (Bidepharm, China).

Study design and settings

The study design was an *in-vitro* experiment for breast cancer cell lines to investigate the impact of $C_{20}H_{13}ClFN_3O$, a pharmacological compound, on breast cancer cell lines MCF-7 and MDA-MB-231 (RRID; CVCL_0062). This study aimed to explore its potential as a therapeutic strategy for breast cancer treatment. As shown in Figure 1, the methodology involved surveying to examine the inhibitory effect of a p38 MAPK inhibitor on MCF-7 and MDA-MB-231 cell lines. This method was conducted by treating the cells with various concentrations of $C_{20}H_{13}ClFN_3O$ and lapatinib, which served as a reference compound. The current study also included determining cell apoptosis and cell cycle assay using flow cytometry. Additionally, the molecular pathway of the interaction between p38 and

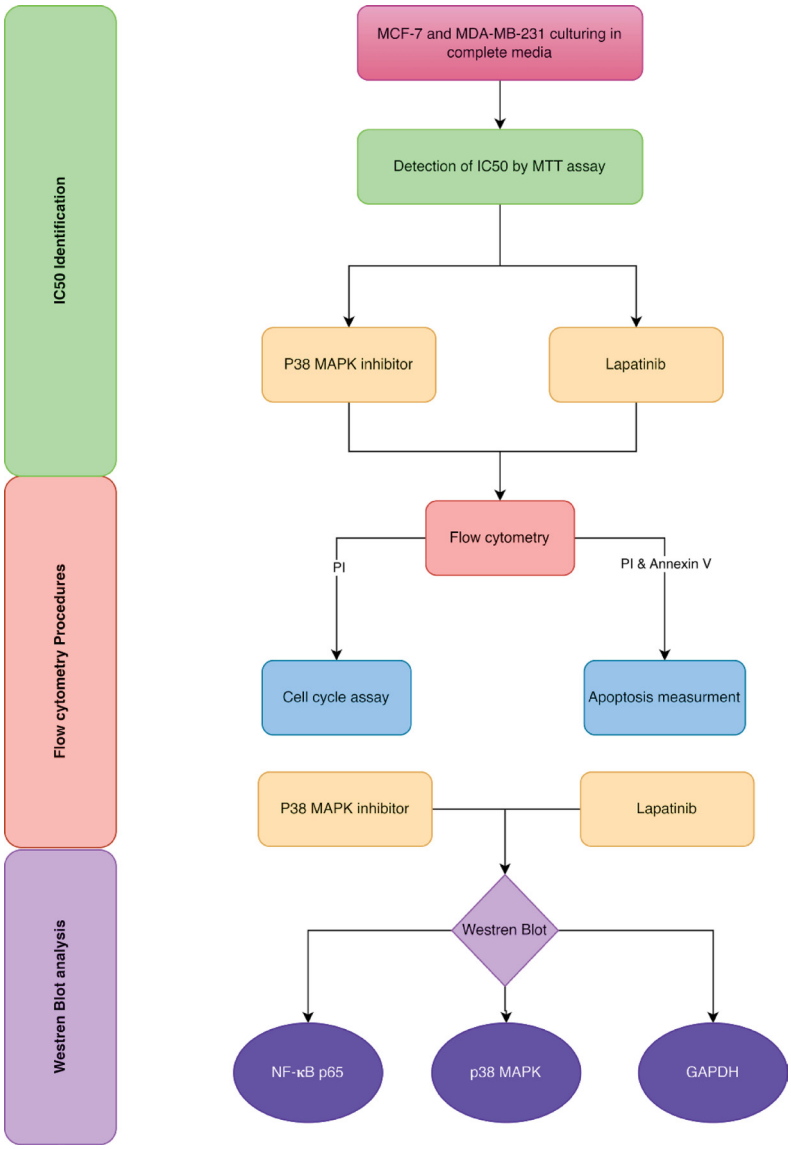

Figure 1. Flow chart of the study.

NF-κB was investigated by estimating protein expression through western blot analysis after treating the cell lines with the $C_{20}H_{13}ClFN_3O$compound.

The *in vitro* experiment was conducted from October 2023 to April 2024 in the Tissue Culture Postgraduate Laboratory of the Pharmacology and Toxicology Department at Mustansiriyah University. Additionally, flow cytometry work was performed in a private laboratory.

Cell lines

The current study utilized two cell lines: MCF-7 and MDA-MB-231. MCF-7 is a human breast cancer cell line that expresses estrogen, progesterone, and glucocorticoid receptors. MCF-7 source is the pleural effusion with metastatic breast cancer. Additionally, MCF-7 is considered a "luminal A" subtype of breast cancer (28).

The MDA-MB-231 cell line, derived from a pleural effusion of a patient with invasive ductal carcinoma, is frequently employed to represent advanced breast cancer. This cell line has negative expression of ER, PR, and E-cadherin. Due to the absence of the growth factor receptor HER2, these cells accurately represent TNBC (29).

Cell culturing

Conventional cell culture procedures were followed in all cell culture activities, including adherence to aseptic techniques to prevent contamination, sterilization of glassware, culturing, subculturing, cryopreservation, thawing, and maintaining cell cultures in a sterile environment. Disposable items and glassware used for tissue culture were autoclaved at 95°C and 1.2 bar pressure for 90 minutes. Cells were cultured in complete high-glucose DMEM (Capricorn Scientific, GmbH) supplemented with 10% FBS (Capricorn Scientific, GmbH) and 1% antibiotic/antimycotic (Capricorn Scientific, GmbH). Cells were seeded at a density of 2×10^3 cells/mL in 75 cm^3 culture flasks and kept in a constant temperature incubator (Hermle, Germany) at 37 °C and 5% CO_2. In addition, cells were sub-cultured to greater than 70% confluence by washing the cell monolayer with PBS (Capricorn Scientific, GmbH) and then incubating with 0.05% trypsin/EDTA (Capricorn Scientific, GmbH) for five minutes. Cells were allowed to detach. Trypsinized cells were re-suspended with a complete medium and isolated by centrifugation in a centrifuge (Hettich, Germany) (30).

Cell proliferation assay

The colorimetric MTT assay is a more convenient method to measure cell viability and proliferation (31). After trypsinization, cell suspensions were prepared and seeded in 100 µL 96-well plates at 3×10^3, 4×10^3, and 5×10^3cells/well and incubated for 24, 48, and 72 hours, respectively. On the day of dosing, $C_{20}H_{13}ClFN_3O$ and lapatinib compound (as a reference) were dissolved in dimethyl sulfoxide (DMSO) (Thomas Baker, India) and serially diluted to produce $C_{20}H_{13}ClFN_3O$ concentrations of 50 µg, 25 µg, 12.5 µg, 6.25 µg, 3.125 µg, 1.5 µg, 1.5 µg, 0.75 µg, 0.32 µg, 0.15 µg, 0.05 µg, and 0.025 µg. When the confluence reaches 80–90%, it is generally considered the best time to treat the cell lines. During the logarithmic growth phase, cells are actively dividing and more responsive to treatment, allowing for a clearer assessment of treatment. To examine the effects on cell proliferation, viability, or other cellular functions, cells were exposed to different concentrations of $C_{20}H_{13}ClFN_3O$ and lapatinib. After incubation, 15 µL of MTT (Bidepharm, Shanghai, China) diluted in PBS was added to each well and incubated at 37 °C for 4 hours. To avoid DMSO crystallization, each well on the plate received 100 µL of solvent at room temperature and in complete darkness. The absorbance corresponding to a standard reference wavelength was measured using a microplate reader (Promega, USA) to measure the optical density at 560 nm (32,33). Three replicates were performed for each treatment.

Annexin V/PI apoptosis assay

The apoptosis rate of the cell lines was determined using the annexin V fluorescein isothiocyanate (FITC) and propidium iodide (PI) apoptosis detection kit (Elabscience, USA).

MCF-7 and MDA-MB-231 cell lines were cultured overnight at a cell density of 1×10^4 per well in six-well plates (two wells for each of the following groups; $C_{20}H_{13}ClFN_3O$, lapatinib, and normal control); normal control was cultured in DMEM. For the MCF-7 cell line, the cells were treated with 5.3 µg $C_{20}H_{13}ClFN_3O$ and 12.5 µg lapatinib compound. For the MDA-MB-231 cell line, the cells were treated with 1.4 µg $C_{20}H_{13}ClFN_3O$, 5.4 µg lapatinib compound (these concentrations were selected based on the results of the MTT test and represent the IC50 of each compound).

After 48 hours, MCF-7 and MDA-MB-231 cell lines were collected, rinsed twice in cold PBS, and then resuspended in 100 µL of binding buffer (1×10^4 cells/mL). 100 µL of MCF-7 and MDA-MB-231 cell lines were mixed with 5 µL of annexin V-FITC and 5 µL of PI. The mixture was incubated at 4 °C for 20 minutes in a dark place. After dilution with 400 µL of binding buffer, the labeled cells were immediately analyzed by flow cytometry (Ex=488 nm; Em=530 nm) (34,35). The stained cells were detected using (BD FACSVerse™), and the data were analyzed using FlowJo 10.2 software (TreeStar, Ashland, OR, USA) (35). Each experiment was performed in duplicate.

Flow cytometry analysis of cell cycle

The basic method of cell cycle flow cytometric analysis is to utilize the changes in DNA content at each stage, which indicates the different stages of cell division (36). Then, 5×10^5 MCF-7 and MDA-MB-231 cell lines were cultured in triplicate in six-well plates, divided into two wells of each group: $C_{20}H_{13}ClFN_3O$, lapatinib, and normal control.

After 24 hours, the cells were treated with 5.3 µg and 10 µg $C_{20}H_{13}ClFN_3O$, 12.5 µg lapatinib compound for the MCF-7 cell line, and 1.4 µg and 2.8 µg $C_{20}H_{13}ClFN_3O$, 5.4 µg lapatinib compound for MDA-B-231 cell line. In addition, after 48 hours, MCF-7 and MDA-MB-231 cell lines were extracted with trypsin, fixed with 1.2mL of anhydrous ethanol, mixed thoroughly, and stored at -20 °C overnight. The fixed cells were centrifuged at 300× gravitational force for five minutes and the supernatant were discarded. Then, 1 mL of PBS was added to re-suspend the cells and stored at room temperature for 15 minutes.

The re-suspended cells were centrifuged at 300×gravitational force for five minutes and the supernatant was discarded. Reagents were added to resuspend the cells except 100 µL of RNase and incubated in a 37 °C water bath for 30 minutes. About 400 µL of PI reagent (50 µg/mL) was added to the re-suspended cells; mixed thoroughly and incubated at 2-8 °C in the dark for 30 minutes. The amount of cellular DNA was determined by flow cytometry using a flow cytometer (USA). A histogram was created to display the results.

p38 and NF-κB protein expressions in breast cancer cell lines by western blot

To prepare cell lysates, cell lines MCF-7 and MDA-MB-231 were seeded to 2 × 10^5 cells/well and cultured in triplicate in six-well plates, divided into two wells of each group; $C_{20}H_{13}ClFN_3O$, lapatinib and normal control; normal control was cultured in DMEM medium and glyceraldehyde-3-phosphate dehydrogenase (GAPDH), a housekeeping protein. Plates were stored at 37 °C and 5% CO_2. After 24 hours, cells were treated with 5.3 µg and 10 µg $C_{20}H_{13}ClFN_3O$, 12.5 µg lapatinib compound for MCF-7 cell line and 1.4 µg and 2.8 µg $C_{20}H_{13}ClFN_3O$, 5.4 µg lapatinib compound for MDA-B-231 cells. After 72 hours, the cell lysis process was performed according to the method described in the western blot detection kit (Elabscience®, USA). The process required washing the cells three times with ice-cold PBS to remove CM. Subsequently, 200 µL of RIPA lysis buffer was added to each well of a 6-well plate, and the plate was placed on ice for 30 minutes to initiate lysis. The cells were then removed from the bottom of the flask with an ice-cold plastic scraper, and the cell suspension was placed in a pre-cooled 1.5 mL Eppendorf tube. At the same time, the sample's viscosity was reduced by sonication in an ice-filled water bath for 1 minute, followed by centrifugation at 12,000 rpm for 10 minutes at 4 °C. Finally, the liquid fraction was collected and stored in a -40 °C refrigerator.

Before electrophoresis, the protein concentration was determined to standardize the distribution of proteins in the gel wells. Excessive amounts of protein can overwhelm the immunodetection process and lead to nonspecific results. Various methods are used to measure the amount of protein. The bicinchoninic acid test (BCA) is commonly used for protein quantification in western blotting (37). The BCA procedure was performed as described in the western blot assay kit (Elabscience®, USA). The procedure began by dissolving 0.563 mg of BSA powder in 1 mL of PBS. The resulting solution was used as a standard protein stock solution and then diluted with PBS to different concentrations (0, 10, 50, 100, 200, 300, 400, and 563 µg/mL). Subsequently, 20 µL of these amounts were added to a 96-well plate in duplicate with unknown samples. The next step was to prepare an apple green BCA working solution by mixing reagent 1 (BCA reagent) with reagent 2 (copper salt solution) in a ratio of 50:1. Each well was then filled with 200µL of the BCA working solution. The plate was then shaken for 20 seconds and incubated in an incubator at 37 °C and 5% CO_2 for 30 minutes. After incubation, the absorbance was measured at 560 nanometers (nm) using a microplate reader (37). The final step was to determine the protein concentration in each cell lysate by applying the following equation:

$$Protein\ concentration\ (\mu g/mL) = (\Delta A562 - b) \div a \times f$$

The obtained optic density (OD) data were then utilized to create the BSA standard curve, as depicted in Figure 2. In which a; the slope of the standard curve, b; the intercept of the standard curve, ΔA562; OD Sample – OD blank,

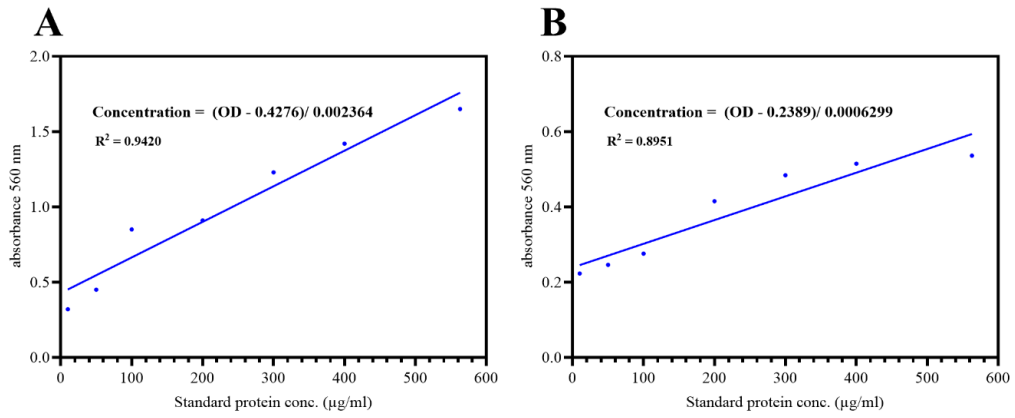

Figure 2. The standard curve for bicinchoninic acid. The linear plot was generated by blotting concentrations of BSA protein on the X-axis against the corresponding OD at 560 nm on the Y-axis. (A) MDA-MB-231, (B) MCF-7

Table 1. The primary and secondary antibodies for western blotting

Target protein	Isotype	Species	Dilution	Supplier
Glyceraldehyde 3-phosphate dehydrogenase	IgG	Rabbit	1:1000	Elabscience, USA
P38	IgG	Rabbit	1:1000	Elabscience, USA
Rabbit IgG	IgG (H+L)-HRP	Goat anti-Rabbit	1:5000	Elabscience, USA
Nuclear factor kappa-B	IgG	Rabbit	1:1000	Elabscience, USA

and f; dilution factor of the sample before the test.

Sample preparation; proteins were extracted from cells and quantified; 5× SDS loading buffer was added to the prepared sample in an Eppendorf tube (4:1 ratio), and the solution was subjected to 95 °C for five minutes using a dry block heater. The proteins are separated based on their molecular weight by SDS-PAGE (SDS-polyacrylamide gel electrophoresis). The gel provides a matrix through which proteins can travel when an electric current is applied. The proteins were transferred using semi-dry transfer from the gel onto a polyvinylidene fluoride membrane (PVDF); this process is facilitated by an electric current that drives the proteins out of the gel onto the membrane. To prevent the non-specific binding of antibodies to the membrane, a blocking buffer (non-fat dry milk) was employed to cover all potential binding sites.

The membrane is incubated with a primary antibody specific to the target protein. After washing away, the unbound primary antibody, a secondary antibody that binds to the primary antibody is added, as shown in Table 1. The presence of the enzyme or fluorescent tag from the secondary antibody is detected using the ChemiDoc™ XRS⁺ imaging system (Bio-Rad Laboratories, France).

Statistical analysis

All statistical analyses of ($C_{20}H_{13}ClFN_3O$) and lapatinib ($C_{29}H_{26}ClFN_4O_4S$) compounds were performed using the GraphPad Prism software 10.2.3. IC_{50} was done by using the nonlinear curve fitting software graph prism pad software. Apoptosis and cell cycle assay were conducted using data comparison between all groups within the same plate by one-way ANOVA with Tukey tests (GraphPad Prism software). The data of the western blot was analyzed using T-test. Values of $P < 0.05$ were considered statistically significant.

Results

Cytotoxicity assay of p38 MAPK inhibitor compound and lapatinib in MCF-7 cell lines

The MCF-7 cells were treated with different concentrations (0.025 µg -50 µg) of ($C_{20}H_{13}ClFN_3O$) and lapatinib ($C_{29}H_{26}ClFN_4O_4S$) compounds. After 72 hours, an MTT assay was performed to analyze the degree of cytotoxicity of these compounds on MCF-7 cell lines. The half maximal inhibitory concentration (IC_{50}) concentration of ($C_{20}H_{13}ClFN_3O$) compound in MCF-7 cells was 5.355 µg and for lapatinib was 12.56 µg (calculated using nonlinear regression analysis), as seen in Figure 3 and Tables 2 and 3.

At a concentration of 6.25 µg for $C_{20}H_{13}ClFN_3O$ compound, there was significantly decreased viability of MCF-7 cells at 24 hours. In contrast, at 72 hours, the viability of MCF-7 cells was reduced at approximately 0.75 µg, indicating that $C_{20}H_{13}ClFN_3O$ compound could suppress the viability of MCF-7 in a dose-dependent manner, as illustrated in Figure 4.

Cytotoxicity assay of p38 MAPK inhibitor compound and lapatinib in MDA-MB-231 cell lines

The MDA-MB-231 cells were treated with different concentrations (0.025 µg-50 µg) of p38 MAPK inhibitor ($C_{20}H_{13}ClFN_3O$) and lapatinib ($C_{29}H_{26}ClFN_4O_4S$) compounds. After 72 hours, an MTT assay was

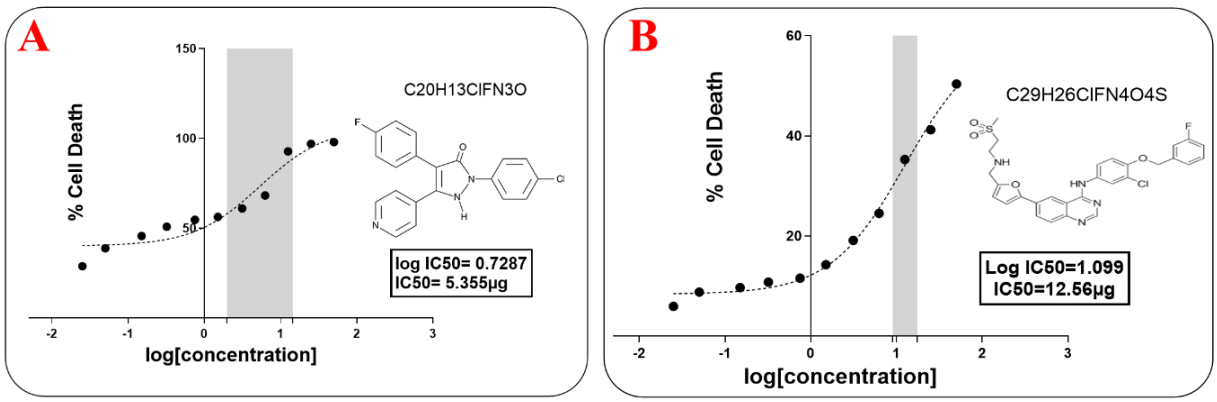

Figure 3. Dose-response curves with IC_{50} for (A) $C_{20}H_{13}ClFN_3O$ and (B) Lapatinib in MCF-7 cells treated for 72 hours with 0.025, 0.05, 0.15, 0.32, 0.75, 1.56, 3.12, 6.25, 12.5, 25 and 50µg dose ranges. The dose-response was plotted over log-transformed concentrations. IC_{50} values were determined using nonlinear regression analysis (Prism Pad 10.2.3). Results represent the mean for triplicate data.

Table 2. The average IC_{50} value, 95% confidence interval, and R^2 for MCF-7 cell line after 72 hours of $C_{20}H_{13}ClFN_3O$ treatment

Incubation time	IC_{50} (µg)	CI at 95% (µg)	R^2
72 hours	5.355	1.973 to 14.54	0.9352

Table 3. The average IC_{50} value, 95% confidence interval, and R^2 for MCF-7 cell line after 72 hours of lapatinib treatment in MCF-7 cell line

Incubation time	IC_{50} (µg)	CI at 95% (µg)	R^2
72 hours	12.56	9.046 to 17.43	0.9937

Table 4. The average IC_{50} value, 95% confidence interval, and R^2 for MDA-MB-231 cell line after 72 hours of $C_{20}H_{13}ClFN_3O$ treatment

Incubation time	IC_{50} (µg)	CI at 95% (µg)	R^2
72 hours	1.419	0.6199 to 3.247	0.9512

Table 5. The average IC_{50} value, 95% confidence interval, and R^2 for MDA-MB-231 cell line after 72 hours of lapatinib treatment

Incubation time	IC_{50} (µg)	CI at 95%(µg)	R^2
72 hours	5.446	4.612 to 6.430	0.9981

performed to analyze the degree of cytotoxicity of these compounds on MCF-7 cell lines. The IC_{50} concentration of ($C_{20}H_{13}ClFN_3O$) compound in MDA-MB-231 cells was 1.419 µg, and for lapatinib, it was 5.446 µg (calculated using nonlinear regression analysis), as seen in Figure 5 and Tables 4 and 5.

To investigate the effect challenging with $C_{20}H_{13}ClFN_3O$ compound, MDA-MB-231 cells were treated with different concentrations 0.025 µg, 0.05 µg, 0.15 µg, 0.32 µg, 0.75 µg, 1.56 µg, 3.12 µg, 6.25 µg, 12.5 µg, 25 µg and 50 µg $C_{20}H_{13}ClFN_3O$ compound for 24, 48 and 72 hours. And showed a reduction of 50% in cell viability at 12.5 µg after 48 hours; however, at the concentrations 6.25 µg, 4.5 µg, and 0.75 µg $C_{20}H_{13}ClFN_3O$ compound for 24, 48 and 72 hours the difference was not statistically significant. The reduction in cell viability became more pronounced after 72 hours with 1.5 µg $C_{20}H_{13}ClFN_3O$ compound, as seen in Figure 6B.

MDA-MB-231 cell lines showed a slight 40% decrease in cell viability after 24 hours compared to 48 and 72 hours in

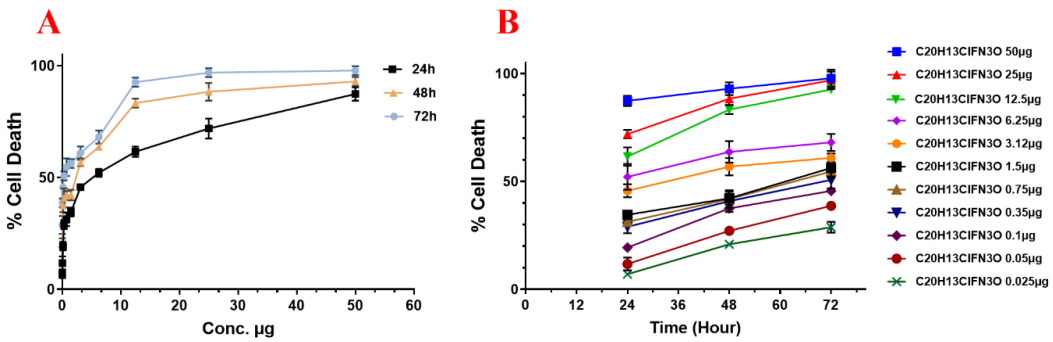

Figure 4. In vitro % cell death of the MCF-7 cells detected by MTT assay. (A) Dose-response curve of $C_{20}H_{13}ClFN_3O$ compound, (B) Time response curve of $C_{20}H_{13}ClFN_3O$ compound. The results of MCF-7 cells post 24, 48 and 72 hours treatment of 3.9, 7.8, 15.6, 31.25, 62.5, 125, 250 and 500 µM $C_{20}H_{13}ClFN_3O$ compound. A microplate reader was measured. The absorbance is at 540 nm (reference wavelength 650 nm). The results represent the mean absorbance ± SEM

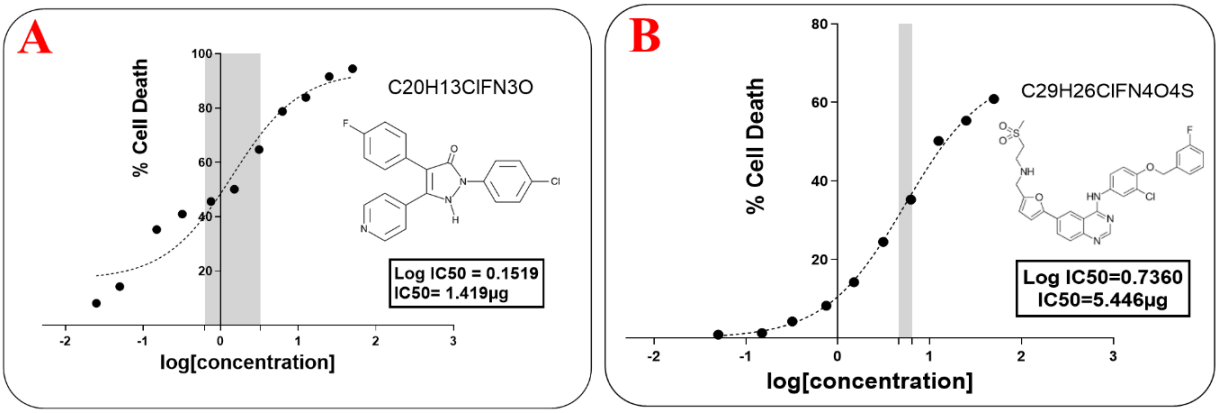

Figure 5. Dose-response curves with IC_{50} for (A) $C_{20}H_{13}ClFN_3O$ and (B) Lapatinib in MDA-MB-231 cells treated for 72 hours with 0.025, 0.05, 0.15, 0.32, 0.75, 1.56, 3.12, 6.25, 12.5, 25 and 50µg dose ranges. The dose-response was plotted over log-transformed concentrations. IC_{50} values were determined using nonlinear regression analysis (Prism Pad 10.2.3). Results represent the mean for triplicate data.

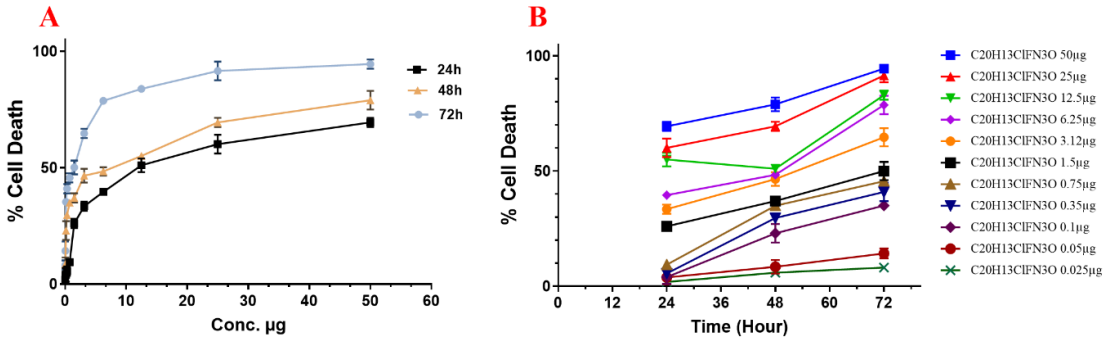

Figure 6. In vitro % cell death of the MDA-MB-231 cells detected by MTT assay. (A) Dose-response curve of $C_{20}H_{13}ClFN_3O$ compound, (B) Time response curve of $C_{20}H_{13}ClFN_3O$ compound. The results of MDA-MB-231 cells post 24, 48 and 72 hours treatment of 3.9, 7.8, 15.6, 31.25, 62.5, 125, 250 and 500µM $C_{20}H_{13}ClFN_3O$ compound. A microplate reader was measured. The absorbance is at 540 nm (reference wavelength 650 nm). The results represent the mean absorbance ± SEM.

high concentrations. In contrast, the cell viability of MDA-MB-231 cells was markedly decreased when treated with 12.5 µg, 25 µg, and 50 µg $C_{20}H_{13}ClFN_3O$ compound after 72 hours (P<0.05). Between the three groups, 72 hours showed a significantly higher percentage of cell death than 24 and 48 hours ($P < 0.05$), as seen in Figure 6A.

In conclusion, the results indicated that these values of IC_{50} of $C_{20}H_{13}ClFN_3O$ compound in two types of breast cancer cell lines (MCF7 and MDA-MB-231; 5.3 µg and 1.4 µg, respectively) are a good value because a low-concentration of $C_{20}H_{13}ClFN_3O$ compound can inhibit the half number of breast cancer cell viability as compared with the IC_{50} of lapatinib (12.5 µg and 5.4 µg) in MCF7 and MDA-MB-231 cell lines.

Measurement of apoptosis by annexin V- FITC/ PI assay

To investigate the effects of the p38 pathway inhibitors on the percentage of breast cancer cell lines apoptotic, FITC annexin V apoptosis by flow cytometry was used. Figure 7 shows a 70% increase in apoptosis in MCF-7 cells treated with 5.3 µg of the compound $C_{20}H_{13}ClFN_3O$ and a 40% increase in apoptosis in cells treated with 12.5 µg of the drug lapatinib, compared to the control group; this increase in apoptosis is statistically significant. Nevertheless, as seen in Figures 7A and B, the proportion of MCF-7 cells undergoing late apoptosis was lower in $C_{20}H_{13}ClFN_3O$ compound at concentration 5.3 µg compared to that achieved by lapatinib (in which 30% of cells achieved late apoptosis). The proportion of apoptotic MDA-MB-231 cells treated with 1.4 µg of $C_{20}H_{13}ClFN_3O$ compound was significantly higher than that of the control group; early apoptosis increased by 23%, and late apoptosis increased by 71%, as seen in Figures 8A and B. Lapatinib at a concentration of 5.4 µg showed a high percentage of late apoptotic cells compared to the control group (75.1%), as seen in Figures 8A and B.

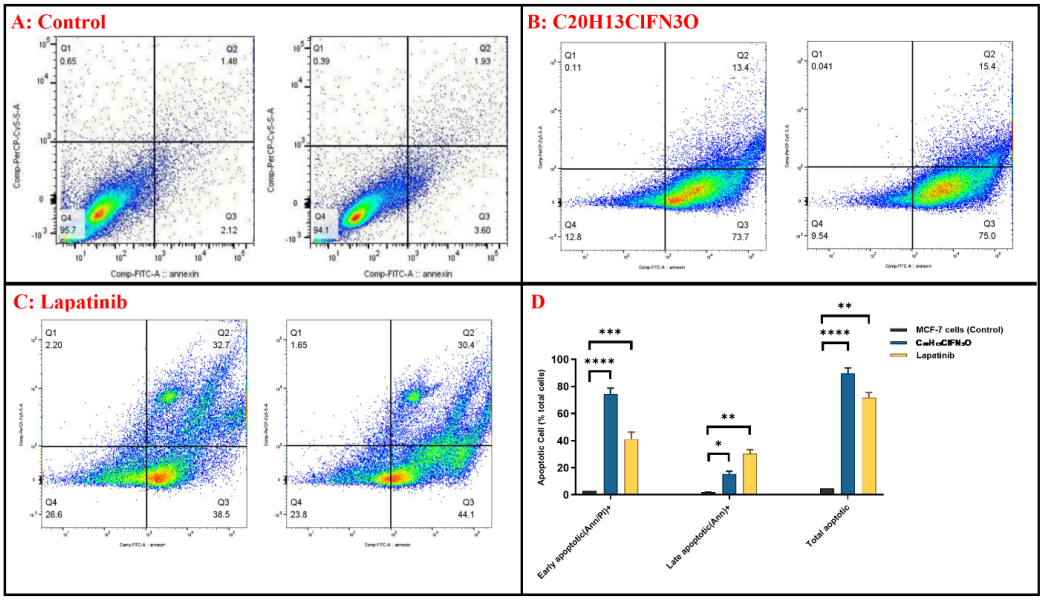

Figure 7. Flow cytometry analysis in MCF-7 cell lines. Effect of (A) Control, (B) $C_{20}H_{13}ClFN_3O$, (C) Lapatinib on the percentage of apoptotic MCF-7 cell lines, the flow cytometry charts illustrating the percentage of live cells (Q4), early apoptotic cells (Q3), late apoptotic cells (Q2) and necrotic cells (Q1) in MCF-7 cells. (D) The statistical bar of the percentage of apoptotic cells presented increased significantly when $C_{20}H_{13}ClFN_3O$ and lapatinib were added. The significant difference compared with untreated cells was p<0.05. The significance was assessed by the one-way ANOVA test.

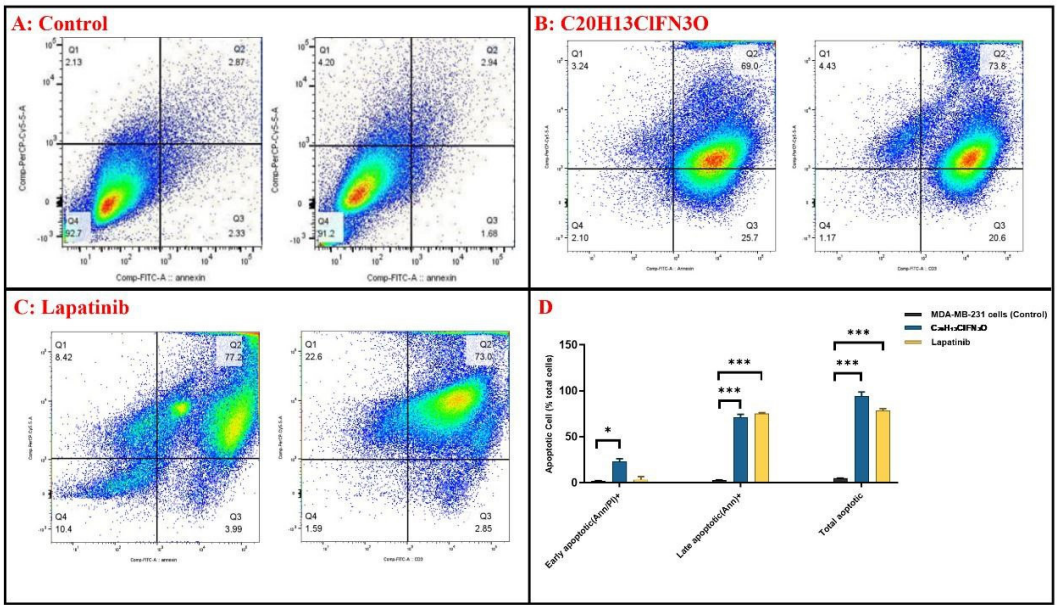

Figure 8. Flow cytometry analysis in MDA-MB-231 cell lines. Effect of (A) Control, (B) $C_{20}H_{13}ClFN_3O$, (C) Lapatinib on the percentage of apoptotic MDA-MB-231 cell lines, the flow cytometry charts illustrating the percentage of live cells (Q4), early apoptotic cells (Q3), late apoptotic cells (Q2) and necrotic cells (Q1) in MDA-MB-231 cells. (D) The statistical bar of the percentage of apoptotic cells presented increased significantly when $C_{20}H_{13}ClFN_3O$ and lapatinib were added. The significant difference compared with untreated cells was $P<0.05$. The significance was assessed by the one-way ANOVA test.

Flow cytometry analysis of cell cycle

To further explore the internal mechanism by which $C_{20}H_{13}ClFN_3O$ compound inhibits the proliferation of MCF-7 cells, the cell cycle distribution of $C_{20}H_{13}ClFN_3O$ compound-treated MCF-7 cells with 5.3 µg and 10 µg $C_{20}H_{13}ClFN_3O$ compound for 48 hours showed an obvious cell cycle arrest at the S phase. In contrast, the 12.5 µg lapatinib compound demonstrated non-significant differences with a control group (Figures 9A and B). The results suggest that the $C_{20}H_{13}ClFN_3O$ compound effectively induces cell cycle arrest at the S phase with increased concentration (5.3 µg and 10 µg).

The effect of the $C_{20}H_{13}ClFN_3O$ compound on the cell cycle in MDA-MB-231 cells showed an obvious cell cycle arrest at the S phase compared with control (Figures 10A and B). The rate of MDA-MB-231 cell lines in the G1 phase at 5.4 µg lapatinib was significantly higher (80%) compared with MDA-MB-231 cells control (61.5%); however, the percentage of G1 phase MDA-MB-231 cells treated with 1.4 µg $C_{20}H_{13}ClFN_3O$ compound was significantly reduced (45%) compared with the control group. These results indicated that the $C_{20}H_{13}ClFN_3O$ compound induces synthesis phase arrest in MDA-MB-231 cells.

The western blot analysis of p38 and NF-κB protein expressions in breast cancer cell lines after treatment with p38 MAPK inhibitor

P38 protein expression

The p38 protein expression in MCF-7 cell lines revealed a significant decrease in its expression relative to glyceraldehyde-3-phosphate dehydrogenase (GAPDH) after treatment of the cells with 5.3 µg of $C_{20}H_{13}ClFN_3O$ compound. Meanwhile, treatment with 12.5 µg lapatinib demonstrated non-significant differences with the control group, as seen in Figure 11.

The p38 protein expression in MDA-MB-231 cell lines revealed a significant decrease in its expression relative to GAPDH after treatment of the cells with 1.4 µg of $C_{20}H_{13}ClFN_3O$ compound. Meanwhile, treatment with 5.4 µg lapatinib demonstrated non-significant differences with the control group, as seen in Figure 12.

NF-κB p65 proteinexpression

As shown in Figures 13A and B, NF-κB p65 expression relative to GAPDH was decreased in MCF-7 cell lines treated with 5.3 µg ($C_{20}H_{13}ClFN_3O$) compound compared to the control group ($P < 0.05$). While MCF-7 cell lines treated with 12.5 µg, lapatinib did not affect the expression of NF-κB p65, suggesting that lapatinib has another pathway to suppress the MCF-7 cell line.

Western blot analysis of NF-κB p65 expression in MDA-MB-231 cell lines (Figures 14A and B) revealed that 1.4 µg ($C_{20}H_{13}ClFN_3O$) and 5.4 µg lapatinib compounds significantly decreased the NF-κB p65 expression relative to GAPDH as compared to the control group ($P<0.05$), suggesting the relationship between p38 and NF-κB p65 proteins.

Discussion

Selecting MCF-7 and MDA-MB-231 cells in this study was to represent different subtypes of breast cancer (MCF-7 as a model for hormone receptor-positive breast cancer, which is a common subtype of breast cancer and MDA-MB-231 cells which lack ERs, progesterone receptors,

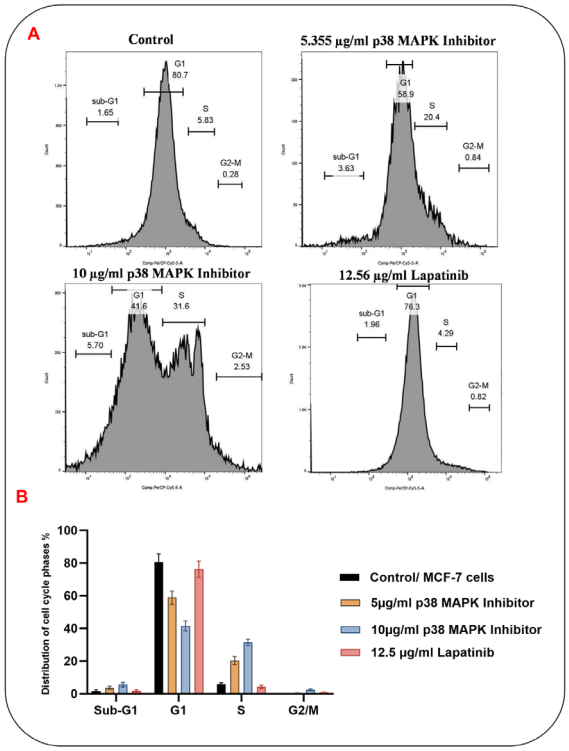

Figure 9. p38 MAPK inhibitor, $C_{20}H_{13}ClFN_3O$, induces cell cycle arrest at the S phase in MCF-7 cells. (a) The cell cycle distribution of p38 MAPK inhibitor-treated MCF-7 cells was measured by flow cytometry. (b) Statistical analysis of the cell cycle distribution of p38 MAPK inhibitor treated MCF-7 cells. All data are expressed as the mean ± SD of three independent experiments. The observed difference is statistically significant when compared to the control group, with a p-value of less than 0.05. The significance was assessed by the one-way ANOVA test.

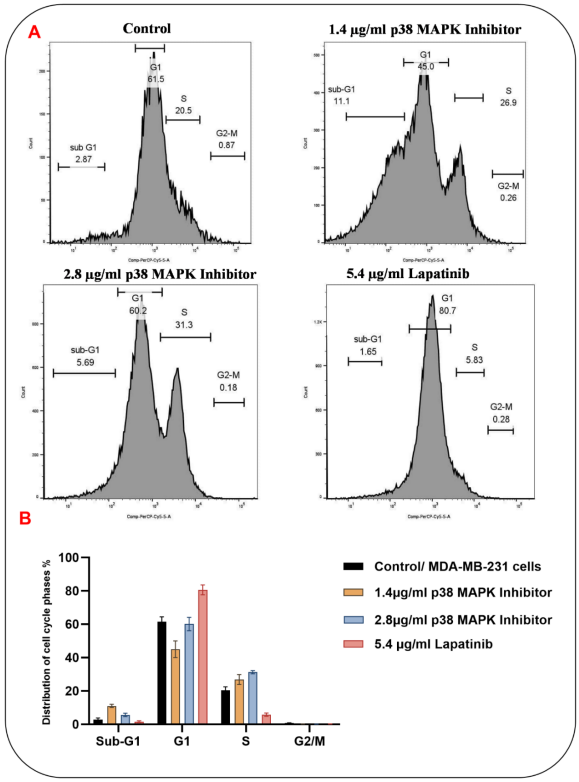

Figure 10. p38 MAPK inhibitor, $C_{20}H_{13}ClFN_3O$, induces cell cycle arrest at the S phase in MDA-MB-231 cells. (a) The cell cycle distribution of p38 MAPK inhibitor-treated MDA-MB-231 cells were measured by flow cytometry. (b) Statistical analysis of the cell cycle distribution of p38 MAPK inhibitor treated MDA-MB-231 cells. All data are expressed as the mean ± SD of three independent experiments. The observed difference is statistically significant when compared to the control group, with a p-value of less than 0.05. The significance was measured by a one-way ANOVA test.

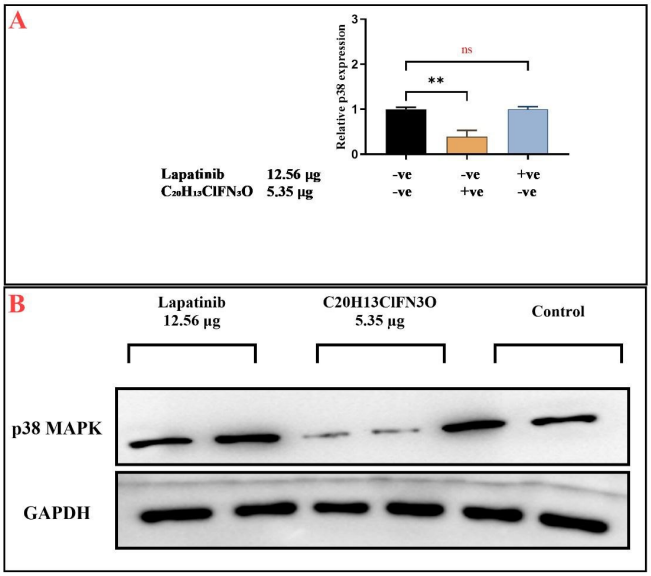

Figure 11. The effect of ($C_{20}H_{13}ClFN_3O$) compound on p38 expression in MCF-7 cells. (A) ($C_{20}H_{13}ClFN_3O$) compound induced decreasing in the p38 expression, and protein bands were measured by ImageJ software; GAPDH was used as the internal control. (B) Cells were treated with ($C_{20}H_{13}ClFN_3O$) compound for 48 h**ours**, and cell lysate was analyzed by western blot. At the bottom, the concentrations of ($C_{20}H_{13}ClFN_3O$) and lapatinib compounds are labeled in (µg). The T-test was conducted to examine the substantial disparities between groups.

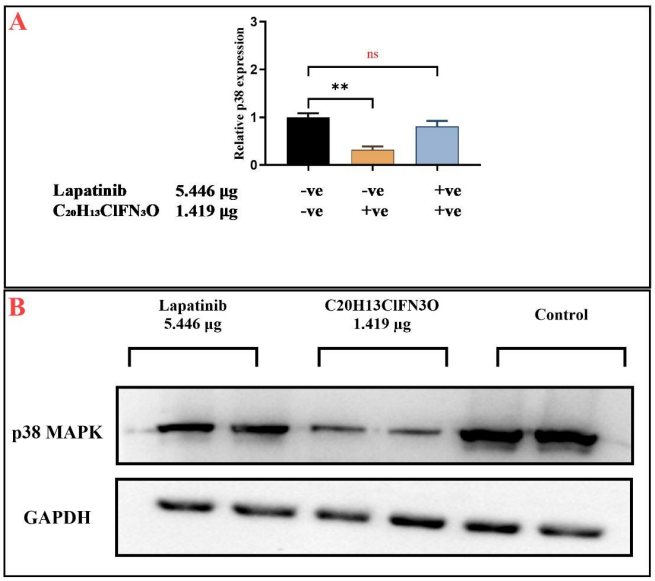

Figure 12. The effect of ($C_{20}H_{13}ClFN_3O$) compound on p38 expression in MDA-MB-231 cells. (A) ($C_{20}H_{13}ClFN_3O$) compound induced decreasing in the p38 expression, and protein bands were measured by ImageJ software; GAPDH was used as an internal control. (B) Cells were treated with ($C_{20}H_{13}ClFN_3O$) for 48 hours, and cell lysate was analyzed by western blot. At the bottom, the concentrations of ($C_{20}H_{13}ClFN_3O$) and lapatinib compounds are labeled in (µg). The T-test was used to examine the substantial disparities between groups.

and HER2, representing a more aggressive and difficult-to-treat subtype of breast cancer), thereby allowing the evaluation of the compound's effectiveness across a spectrum of breast cancer type. The involvement of p38 MAPK in cancer is intricate, and the results are somewhat conflicting, contingent on various systems and situations. Nevertheless, an increasing body of research indicates the potential use of $C_{20}H_{13}ClFN_3O$ for the treatment of cancer-related illnesses. Additional *in-vivo* and clinical research is necessary to gather further information about the possible therapeutic application of $C_{20}H_{13}ClFN_3O$ for cancer treatment. This is based on the existing evidence that demonstrates the inhibitory effect of $C_{20}H_{13}ClFN_3O$ on cancer cell proliferation, invasion, and migration in vitro. The p38 MAPK-signaling pathway is involved in cell proliferation, apoptosis, and cellular motility, promoting cell migration, tumor invasion, and metastasis. In breast cancer patients, high levels of p38 have been correlated with highly invasive and poor prognostic breast cancer (38-40). Depending on the nature of the stimuli and the

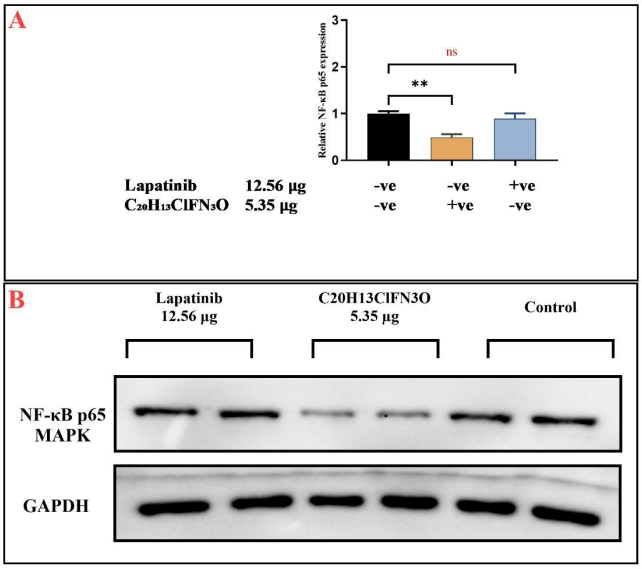

Figure 13. The effect of ($C_{20}H_{13}ClFN_3O$) compound on NF-κB p65 expression in MCF-7 cells. (A) ($C_{20}H_{13}ClFN_3O$) compound induced decreasing in the NF-κB p65 expression, and protein bands were measured by ImageJ software; GAPDH was used as the internal control. (B) Cells were treated with ($C_{20}H_{13}ClFN_3O$) compound for 48 hours, and cell lysate was analyzed by western blot. At the bottom, the concentrations of ($C_{20}H_{13}ClFN_3O$) and lapatinib compounds are labeled in (µg). The T-test was conducted to examine the substantial disparities between groups.

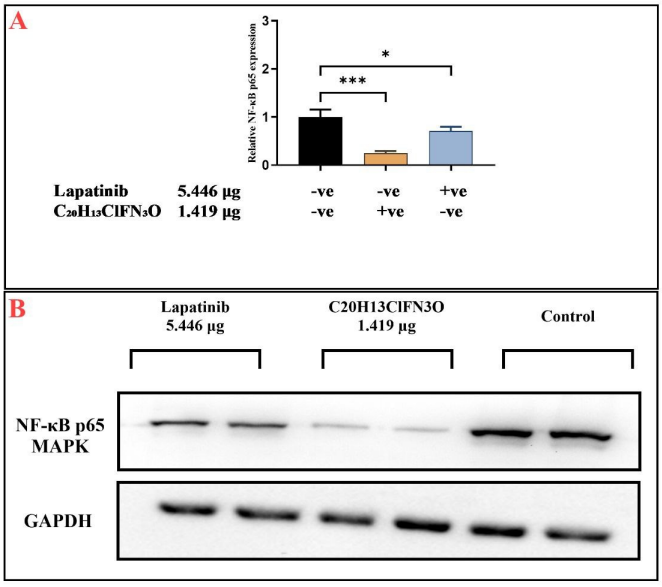

Figure 14. The effect of ($C_{20}H_{13}ClFN_3O$) compound on NF-κB p65 expression in MDA-MB-231 cells. (A) ($C_{20}H_{13}ClFN_3O$) compound induced decreasing in the NF-κB p65 expression, and protein bands were measured by ImageJ software; GAPDH was used as an internal control. (B) Cells were treated with ($C_{20}H_{13}ClFN_3O$) compound for 48 hours, and cell lysate was analyzed by western blot. At the bottom, the concentrations of ($C_{20}H_{13}ClFN_3O$) and lapatinib compounds are labeled in (µg). The T-test was conducted to examine the substantial disparities between groups.

cellular context, p38 can mediate a wide variety of cellular responses. p38 induces apoptosis in some cells (41,42), but prevents apoptosis in others (43,44). Likewise, p38 exhibits opposing effects on cell cycle regulation (45). p38 is involved in cell proliferation and tumorigenesis. Conversely, several studies have implicated p38 as a negative regulator of cell proliferation (46). The reasons for such discrepancy in p38's role are still unclear. The role of p38 in TNBC progression is multifaceted and involves various pathways that contribute to cell proliferation, survival, apoptosis, inflammation and stress responses. In addition to the p38 MAPK pathway can crosstalk with another pathway in TNBC: c-Jun N-terminal kinase (JNK) pathway, NF-κB Pathway, Akt/PI3K pathway, ERK/MAPK pathway, stress response pathways, and hypoxia-inducible factor (HIF) pathway (47).

The role of NF-κB p65 inhibition in breast cancer suppression was NF-κB p65, which is known to promote the expression of anti-apoptotic genes; thereby, inhibiting NF-κB p65 can lead to increased apoptosis in cancer cells.

Also, inhibition can reduce inflammation and inhibition of proliferation. So inhibiting this pathway can slow down or halt tumor growth (48). NF-κB p65 controls the expression of genes involved in cell migration and invasion. Its inhibition can reduce the metastatic potential of breast cancer cells (49). Possible ways that p38 inhibition decreases the expression of NF-κB by inhibition of IKK activation because p38 MAPK activates IκB kinase (IKK), which phosphorylates IκBα (inhibitor of nuclear factor kappa B), leading to its degradation and subsequent activation of NF-κB. Inhibiting p38 MAPK can prevent this activation cascade. P38 MAPK interacts with other signaling pathways, such as JNK and ERK, which can indirectly affect NF-κB activity (50). The western blot findings in this study showed that the p38 protein was overexpressed in MCF-7 and MDA-MB-231 cells. After treating the MCF-7 cell with 5.3 µg $C_{20}H_{13}ClFN_3O$ compound and treating MDA-MB-231 with 1.4 µg $C_{20}H_{13}ClFN_3O$ compound, the expression of the p38 protein was decreased much greater than the downregulation by lapatinib. Additionally, NF-κB p65 protein expression was downregulated in MCF-7 and MDA-MB-231 cells after treatment with $C_{20}H_{13}ClFN_3O$ compound. When p38 and NF-κB p65 protein were downregulated, the proliferation of MCF-7 and MDA-MB-231 cells was inhibited in a time and dose-dependent manner, according to the MTT results. These findings suggest that the $C_{20}H_{13}ClFN_3O$ compound exerts a powerful anti-proliferative effect on breast cancer cell lines via the downregulation of p38 and NF-κB p65 protein. The potential mechanisms by which the $C_{20}H_{13}ClFN_3O$ inhibits p38 and NF-κB, by apoptosis induction could be increased apoptosis in breast cancer cells. Inhibition of metastasis by p38 MAPK inhibitors which reduce the metastatic potential of breast cancer cells by affecting cell migration and invasion and chemotherapy sensitization by inhibiting p38 MAPK, breast cancer cells can become more sensitive to chemotherapy agents, potentially overcoming resistance mechanisms (51,52). The cytotoxicity results presented here agree with a previous study, which revealed that p38 MAPK inhibitors (SB203580 and SB202190) showed an anti-proliferative effect on MDA-MB-231 cells via downregulation of phosphorylation of ERK1/2 (ERK1/2 pathway has been known to regulate NF-κB activation as well (53), and increased Ser15 phosphorylation of mutant p53 (R280K) (the activation of wild-type p53 has been shown to inhibit NF-κB) (54). A previous study examined SB203580 in MDA-MB-231 cells, which was treated with LyeTx II, which is capable of increasing MDA-MB-231 aggressive breast cancer cell proliferation, SB203580 downregulate p38 and NF-κB pathways (55). A previous study that examined inhibitors of ERK1/2 (PD0325901), p38 MAPK (SB203580), and PI3K (LY294002) preferentially reduced breast cancer cell proliferation in MCF-7 cells (56). Chen et al used small molecule inhibitors to assess the effect of inhibiting p38 (p38α isoform) on breast cancer cell proliferation; they concluded that targeting p38 resulted in an antiproliferative effect on MDA-MB-468 cells (57).

Flow cytometry validated the observed cell cycle disruptions and examined the intracellular processes responsible for these abnormalities. The p38 MAPK protein functions as a suppressor of cell cycle advancement. The flow cytometry results on the cell cycle assay of this study showed that the compound $C_{20}H_{13}ClFN_3O$ inhibits p38 and increases the apoptosis rate of MCF-7 and MDA-MB-231 cells. In MCF-7 cells treated with 5.3 µg and 10 µg $C_{20}H_{13}ClFN_3O$ compound for 48 hours, there was an obvious cell cycle arrest at the S (synthesis) phase.

It is worth mentioning that the effect of the $C_{20}H_{13}ClFN_3O$ compound on the cell cycle in MDA-MB-231 cells depended upon the dose increasing because the results revealed an increased percentage of cells in the synthesis phase among MDA-MB-231 cells at 1.4 µg and 2.8 µg $C_{20}H_{13}ClFN_3O$ compound compared with control (Figure 10A and B). The rate of MDA-MB-231 cell lines in the G1 phase at 5.4 µg lapatinib was significantly higher (80%) compared with MDA-MB-231 cells control (61.5%); however, the percentage of G1 (first gap phase) phase MDA-MB-231 cells treated with 1.4 µg $C_{20}H_{13}ClFN_3O$ compound was significantly reduced (45%) compared with the control group ($P<0.05$). These results indicated that the $C_{20}H_{13}ClFN_3O$ compound induces S phase arrest in MDA-MB-231 cells.

Additionally, the current study examined the FITC-annexin V apoptosis by flow cytometry; it showed that treating the MCF-7 cells with 5.3 µg $C_{20}H_{13}ClFN_3O$ compound led to increased early apoptotic by 70% (compared to 40% after treatment with 12.5 µg lapatinib), while the efficacy of $C_{20}H_{13}ClFN_3O$ compound was less than lapatinib in inducing late apoptosis (15% vs. 30%) in MCF-7 cells. In MDA-MB-231 cells, only the $C_{20}H_{13}ClFN_3O$ compound exerted a significant early apoptotic effect (23%), while lapatinib did not show a significant apoptotic effect compared to the control, $C_{20}H_{13}ClFN_3O$ compound showed strong late apoptotic effect (71%).

The intricate interplay between cell survival and cell death is multifaceted, and extensive research is being conducted to comprehend how tumor cells govern the pivotal junctures between these pathways. Numerous anticancer drugs that have demonstrated clinical efficacy have been found to elicit apoptosis in tumor cells (58), and this mechanism is thought to be a significant factor in their therapeutic activities. The specific pathways through which these drugs induce apoptosis in cancer cells have been reported to be diverse and contingent upon both the characteristics of the drug and the genetic background and origin of the tumor (59). The limitations of this study were only performed on cell lines (*in-vitro*) and was not examined on an animal model (*in-vivo*) and conducted on breast cancer cell lines and was not performed on normal breast cells to determine the cytotoxicity effect

of the $C_{20}H_{13}ClFN_3O$ compound on healthy cells. Hence, suggestions for further studies on this subject by studying the cytotoxic activity of the $C_{20}H_{13}ClFN_3O$ compound on normal cell lines, evaluating the cytotoxic activity of the $C_{20}H_{13}ClFN_3O$ compound on other types of breast cancer cell lines. Study the effect of the $C_{20}H_{13}ClFN_3O$ on other specific parameters involved in the migration activity of metastasis in breast cancer cells and evaluate the impact of the $C_{20}H_{13}ClFN_3O$ compound in animal models (*in-vivo*) to assess its efficacy.

Conclusion

The findings of this study indicate that p38 pathway inhibition by $C_{20}H_{13}ClFN_3O$ *in-vitro* can decrease the expression of p38 MAPK and NF-kB p65, induce apoptosis, and suppress breast cancer cell growth. Overall, the p38 MAPK-signaling pathway plays a crucial role in facilitating the malignant growth, invasion, and metastasis of breast cancer. While the exact process is not yet understood, targeting an inhibitor of the MAPK-signaling pathway is a new and promising approach for cancer intervention techniques. Our findings indicate that targeting the p38 MAPK-signaling pathway could be a promising therapeutic approach for treating breast cancer.

Limitations of the study

The current study has some limitations that include:

1. 1. This study was only performed on cell lines (*in-vitro*) and was not examined on an animal model (in *vivo*), restricting the applicability of the findings to whole organisms.
2. 2. This study was only conducted on breast cancer cell lines and not performed on normal breast cells to determine the cytotoxicity effect of the $C_{20}H_{13}ClFN_3O$ compound on healthy cells.

Acknowledgments

The authors thank the College of Pharmacy – Mustansiriyah University (www.uomustansiriyah.edu.iq), Baghdad, Iraq, for supporting this work.

Authors' contribution

Conceptualization: Mustafa Abduljabbar A-qader. Intesar Tarik Numan.
Data curation: Mustafa Abduljabbar A-qader.
Formal analysis: Intesar Tarik Numan, Basma Talib Al-Sudani.
Funding acquisition: Intesar Tarik Numan, Basma Talib Al-Sudani.
Investigation: Mustafa Abduljabbar A-qader, Basma Talib Al-Sudani.
Methodology: Mustafa Abduljabbar A-qader, Intesar Tarik Numan.
Project administration: Mustafa Abduljabbar A-qader.
Resources: Basma Talib Al-Sudani.
Software: Mustafa Abduljabbar A-qader Basma Talib Al-Sudani.
Supervision: Intesar Tarik Numan Basma Talib Al-Sudani.
Validation: Mustafa Abduljabbar A-qader.
Visualization: Mustafa Abduljabbar A-qader Basma Talib Al-Sudani.
Writing–original draft: Mustafa Abduljabbar A-qader, Intesar Tarik Numan.
Writing–review & editing: Mustafa Abduljabbar A-qader.

Conflicts of interest

The authors declare that they have no competing interests.

Ethical issues

The research adhered to the principles outlined in the Declaration of Helsinki. This study was approved by the ethics committee of Mustansiriyah University/Pharmacy College, Pharmacology and Toxicology Department, Baghdad-Iraq. This study was extracted from the MSc, thesis of Mustafa Abduljabbar A-qader at this university. Besides, ethical issues (including plagiarism, data fabrication, and double publication) have been completely observed by the authors.

Funding/Support

This research did not receive any specific grant from funding agencies in the public, commercial, or not-for-profit sectors.

References

1. Evaluation of anti-proliferative activity of simvastatin and atorvastatin on MCF7 cell line compared with doxorubicin using MTT test. Al Mustansiriyah J Pharm Sci. 2018;18:163-9.
2. Watkins EJ. Overview of breast cancer. JAAPA. 2019;32:13-17. doi: 10.1097/01.JAA.0000580524.95733.3d.
3. Sung H, Ferlay J, Siegel RL, Laversanne M, Soerjomataram I, Jemal A, et al. Global Cancer Statistics 2020: GLOBOCAN Estimates of Incidence and Mortality Worldwide for 36 Cancers in 185 Countries. CA Cancer J Clin. 2021;71:209-249. doi: 10.3322/caac.21660.
4. Al-Hashimi MMY. Trends in Breast Cancer Incidence in Iraq During the Period 2000-2019. Asian Pac J Cancer Prev. 2021;22:3889-3896. doi: 10.31557/APJCP.2021.22.12.3889.
5. Torre LA, Bray F, Siegel RL, Ferlay J, Lortet-Tieulent J, Jemal A. Global cancer statistics, 2012. CA Cancer J Clin. 2015;65:87-108. doi: 10.3322/caac.21262.
6. Guo J, Luo C, Yang Y, Dong J, Guo Z, Yang J, et al. MiR-491-5p, as a Tumor Suppressor, Prevents Migration and Invasion of Breast Cancer by Targeting ZNF-703 to Regulate AKT/mTOR Pathway. Cancer Manag Res. 2021;13:403-413. doi: 10.2147/CMAR.S279747.
7. Chaffer CL, Weinberg RA. A perspective on cancer cell metastasis. Science. 2011;331:1559-64. doi: 10.1126/science.1203543.
8. Lanigan F, O'Connor D, Martin F, Gallagher WM. Molecular links between mammary gland development and breast cancer. Cell Mol Life Sci. 2007;64:3159-84. doi: 10.1007/s00018-007-7386-2.
9. Garrido-Castro AC, Lin NU, Polyak K. Insights into Molecular Classifications of Triple-Negative Breast Cancer: Improving Patient Selection for Treatment. Cancer Discov. 2019;9:176-198. doi: 10.1158/2159-8290.CD-18-1177.
10. Yao H, He G, Yan S, Chen C, Song L, Rosol TJ, et al. Triple-negative breast cancer: is there a treatment on the horizon? Oncotarget. 2017;8:1913-1924. doi: 10.18632/oncotarget.12284.
11. Geyer FC, Pareja F, Weigelt B, Rakha E, Ellis IO, Schnitt SJ, et al. The Spectrum of Triple-Negative Breast Disease: High- and Low-Grade Lesions. Am J Pathol. 2017;187:2139-2151. doi: 10.1016/j.ajpath.2017.03.016.
12. André F, Zielinski CC. Optimal strategies for the treatment of metastatic triple-negative breast cancer with currently approved agents. Ann Oncol. 2012;23 Suppl 6:vi46-51. doi: 10.1093/annonc/mds195.
13. Pearson G, Robinson F, Beers Gibson T, Xu BE, Karandikar M, Berman K, Cobb MH. Mitogen-activated protein (MAP) kinase pathways: regulation and physiological functions. Endocr Rev. 2001;22:153-83. doi: 10.1210/edrv.22.2.0428.
14. Qi M, Elion EA. MAP kinase pathways. J Cell Sci.

2005;118:3569-72. doi: 10.1242/jcs.02470.
15. Morales-Martínez M, Vega MI. p38 Molecular Targeting for Next-Generation Multiple Myeloma Therapy. Cancers (Basel). 2024;16:256. doi: 10.3390/cancers16020256.
16. Son SH, Lee NR, Gee MS, Song CW, Lee SJ, Lee SK, et al. Chemical Knockdown of Phosphorylated p38 Mitogen-Activated Protein Kinase (MAPK) as a Novel Approach for the Treatment of Alzheimer's Disease. ACS Cent Sci. 2023;9:417-426. doi: 10.1021/acscentsci.2c01369.
17. Zhang Y, Yang WK, Wen GM, Tang H, Wu CA, Wu YX, et al. High expression of PRKDC promotes breast cancer cell growth via p38 MAPK signaling and is associated with poor survival. Mol Genet Genomic Med. 2019;7:e908. doi: 10.1002/mgg3.908.
18. Zhang T, Ma C, Zhang Z, Zhang H, Hu H. NF-κB signaling in inflammation and cancer. MedComm (2020). 2021;2:618-653. doi: 10.1002/mco2.104.
19. Paul A, Edwards J, Pepper C, Mackay S. Inhibitory-κB Kinase (IKK) α and Nuclear Factor-κB (NFκB)-Inducing Kinase (NIK) as Anti-Cancer Drug Targets. Cells. 2018;7:176. doi: 10.3390/cells7100176.
20. Guo Q, Jin Y, Chen X, Ye X, Shen X, Lin M, et al. NF-κB in biology and targeted therapy: new insights and translational implications. Signal Transduct Target Ther. 2024;9:53. doi: 10.1038/s41392-024-01757-9.
21. Shih VF, Tsui R, Caldwell A, Hoffmann A. A single NFκB system for both canonical and non-canonical signaling. Cell Res. 2011;21:86-102. doi: 10.1038/cr.2010.161.
22. Song W, Mazzieri R, Yang T, Gobe GC. Translational Significance for Tumor Metastasis of Tumor-Associated Macrophages and Epithelial-Mesenchymal Transition. Front Immunol. 2017;8:1106. doi: 10.3389/fimmu.2017.01106.
23. Sau A, Lau R, Cabrita MA, Nolan E, Crooks PA, Visvader JE, et al. Persistent Activation of NF-κB in BRCA1-Deficient Mammary Progenitors Drives Aberrant Proliferation and Accumulation of DNA Damage. Cell Stem Cell. 2016;19:52-65. doi: 10.1016/j.stem.2016.05.003.
24. Saha RN, Jana M, Pahan K. MAPK p38 regulates transcriptional activity of NF-kappaB in primary human astrocytes via acetylation of p65. J Immunol. 2007;179:7101-9. doi: 10.4049/jimmunol.179.10.7101.
25. Craig R, Larkin A, Mingo AM, Thuerauf DJ, Andrews C, McDonough PM, et al. p38 MAPK and NF-kappa B collaborate to induce interleukin-6 gene expression and release. Evidence for a cytoprotective autocrine signaling pathway in a cardiac myocyte model system. J Biol Chem. 2000;275:23814-24. doi: 10.1074/jbc.M909695199.
26. Barton BE. Interleukin-6 and new strategies for the treatment of cancer, hyperproliferative diseases and paraneoplastic syndromes. Expert Opin Ther Targets. 2005;9:737-52. doi: 10.1517/14728222.9.4.737.
27. Saha RN, Jana M, Pahan K. MAPK p38 regulates transcriptional activity of NF-kappaB in primary human astrocytes via acetylation of p65. J Immunol. 2007;179:7101-9. doi: 10.4049/jimmunol.179.10.7101.
28. Shammout ODA, Ashmawy NS, Shakartalla SB, Altaie AM, Semreen MH, Omar HA, et al. Comparative sphingolipidomic analysis reveals significant differences between doxorubicin-sensitive and -resistance MCF-7 cells. PLoS One. 2021;16:e0258363. doi: 10.1371/journal.pone.0258363.
29. Zeng L, Li W, Chen CS. Breast cancer animal models and applications. Zool Res. 2020;41:477-494. doi: 10.24272/j.issn.2095-8137.2020.095.
30. Weiskirchen S, Schröder SK, Buhl EM, Weiskirchen R. A Beginner's Guide to Cell Culture: Practical Advice for Preventing Needless Problems. Cells. 2023;12:682. doi: 10.3390/cells12050682.
31. Adan A, Kiraz Y, Baran Y. Cell Proliferation and Cytotoxicity Assays. Curr Pharm Biotechnol. 2016;17:1213-1221. doi: 10.2174/1389201017666160808160513.
32. Stockert JC, Horobin RW, Colombo LL, Blázquez-Castro A. Tetrazolium salts and formazan products in Cell Biology: Viability assessment, fluorescence imaging, and labeling perspectives. Acta Histochem. 2018;120:159-167. doi: 10.1016/j.acthis.2018.02.005.
33. Cytotoxicity of Cryptochlorogenic acid against Breast cancer cell line (MCF7) isolated from Moringa oleifera Leaves Cultivated in Iraq. Al Mustansiriyah J Pharmaceutical Sci. 2022;22:35-43.
34. Crowley LC, Marfell BJ, Scott AP, Waterhouse NJ. Quantitation of Apoptosis and Necrosis by Annexin V Binding, Propidium Iodide Uptake, and Flow Cytometry. Cold Spring Harb Protoc. 2016;2016. doi: 10.1101/pdb.prot087288.
35. Telford W, Tamul K, Bradford J. Measurement and Characterization of Apoptosis by Flow Cytometry. Curr Protoc Cytom. 2016;77:9.49.1-9.49.28. doi: 10.1002/cpcy.1.
36. Kim KH, Sederstrom JM. Assaying Cell Cycle Status Using Flow Cytometry. Curr Protoc Mol Biol. 2015;111:28.6.1-28.6.11. doi: 10.1002/0471142727.mb2806s111.
37. Mishra V. Dot-Blotting: A Quick Method for Expression Analysis of Recombinant Proteins. Curr Protoc. 2022;2:e546. doi: 10.1002/cpz1.546.
38. Salh B, Marotta A, Wagey R, Sayed M, Pelech S. Dysregulation of phosphatidylinositol 3-kinase and downstream effectors in human breast cancer. Int J Cancer. 2002;98:148-54. doi: 10.1002/ijc.10147.
39. Davidson B, Konstantinovsky S, Kleinberg L, Nguyen MT, Bassarova A, Kvalheim G, et al. The mitogen-activated protein kinases (MAPK) p38 and JNK are markers of tumor progression in breast carcinoma. Gynecol Oncol. 2006;102:453-61. doi: 10.1016/j.ygyno.2006.01.034.
40. Holliday DL, Speirs V. Choosing the right cell line for breast cancer research. Breast Cancer Res. 2011;13:215. doi: 10.1186/bcr2889.
41. Baines CP, Molkentin JD. STRESS signaling pathways that modulate cardiac myocyte apoptosis. J Mol Cell Cardiol. 2005;38:47-62. doi: 10.1016/j.yjmcc.2004.11.004.
42. Bulavin DV, Higashimoto Y, Popoff IJ, Gaarde WA, Basrur V, Potapova O, et al. Initiation of a G2/M checkpoint after ultraviolet radiation requires p38 kinase. Nature. 2001;411:102-7. doi: 10.1038/35075107.
43. Hendrickx N, Volanti C, Moens U, Seternes OM, de Witte P, Vandenheede JR, et al. Up-regulation of cyclooxygenase-2 and apoptosis resistance by p38 MAPK in hypericin-mediated photodynamic therapy of human cancer cells. J Biol Chem. 2003;278:52231-9. doi: 10.1074/jbc.M307591200.
44. Kocanova S, Buytaert E, Matroule JY, Piette J, Golab J, de Witte P, et al. Induction of heme-oxygenase 1 requires the p38MAPK and PI3K pathways and suppresses apoptotic cell death following hypericin-mediated photodynamic therapy. Apoptosis. 2007;12:731-41. doi: 10.1007/s10495-006-0016-x.
45. Zarubin T, Han J. Activation and signaling of the p38 MAP kinase pathway. Cell Res. 2005;15:11-8. doi: 10.1038/sj.cr.7290257.
46. Lavoie JN, L'Allemain G, Brunet A, Müller R, Pouysségur J. Cyclin D1 expression is regulated positively by the p42/p44MAPK and negatively by the p38/HOGMAPK pathway. J Biol Chem. 1996;271:20608-16. doi: 10.1074/jbc.271.34.20608.
47. Yang JY, Hung MC. A new fork for clinical application: targeting forkhead transcription factors in cancer. Clin Cancer Res. 2009

Feb 1;15:752-7. doi: 10.1158/1078-0432.CCR-08-0124.
48. DiDonato JA, Mercurio F, Karin M. NF-κB and the link between inflammation and cancer. Immunol Rev. 2012;246:379-400. doi: 10.1111/j.1600-065X.2012.01099.x.
49. Park MH, Hong JT. Roles of NF-κB in Cancer and Inflammatory Diseases and Their Therapeutic Approaches. Cells. 2016;5:15. doi: 10.3390/cells5020015.
50. Hoesel B, Schmid JA. The complexity of NF-κB signaling in inflammation and cancer. Mol Cancer. 2013 2;12:86. doi: 10.1186/1476-4598-12-86.
51. Wagner EF, Nebreda AR. Signal integration by JNK and p38 MAPK pathways in cancer development. Nat Rev Cancer. 2009;9:537-49. doi: 10.1038/nrc2694.
52. Pettus LH, Wurz RP. Small molecule p38 MAP kinase inhibitors for the treatment of inflammatory diseases: novel structures and developments during 2006-2008. Curr Top Med Chem. 2008;8:1452-67. doi: 10.2174/156802608786264245.
53. Kim BM, Kim DH, Park JH, Surh YJ, Na HK. Ginsenoside Rg3 Inhibits Constitutive Activation of NF-κB Signaling in Human Breast Cancer (MDA-MB-231) Cells: ERK and Akt as Potential Upstream Targets. J Cancer Prev. 2014;19:23-30. doi: 10.15430/jcp.2014.19.1.23.
54. O'Neill EJ, Termini D, Albano A, Tsiani E. Anti-Cancer Properties of Theaflavins. Molecules. 2021 Feb 13;26:987. doi: 10.3390/molecules26040987. PMID: 33668434; PMCID: PMC7917939.
55. Huth HW, Santos DM, Gravina HD, Resende JM, Goes AM, de Lima ME, et al. Upregulation of p38 pathway accelerates proliferation and migration of MDA-MB-231 breast cancer cells. Oncol Rep. 2017;37:2497-2505. doi: 10.3892/or.2017.5452.
56. Khajah MA, Mathew PM, Luqmani YA. Inhibitors of PI3K/ERK1/2/p38 MAPK Show Preferential Activity Against Endocrine-Resistant Breast Cancer Cells. Oncol Res. 2017;25:1283-1295. doi: 10.3727/096504017X14883245308282.
57. Chen L, Mayer JA, Krisko TI, Speers CW, Wang T, Hilsenbeck SG, et al. Inhibition of the p38 kinase suppresses the proliferation of human ER-negative breast cancer cells. Cancer Res. 2009;69:8853-61. doi: 10.1158/0008-5472.CAN-09-1636.
58. Sidi S, Sanda T, Kennedy RD, Hagen AT, Jette CA, Hoffmans R, et al. Chk1 suppresses a caspase-2 apoptotic response to DNA damage that bypasses p53, Bcl-2, and caspase-3. Cell. 2008;133:864-77. doi: 10.1016/j.cell.2008.03.037.
59. Carneiro BA, El-Deiry WS. Targeting apoptosis in cancer therapy. Nat Rev Clin Oncol. 2020;17:395-417. doi: 10.1038/s41571-020-0341-y.